Hot Pixel Behavior as Pixel Size Reduces to 1 micron

Glenn H. Chapman, Rahul Thomas
School of Engineering Science
Simon Fraser University
Burnaby, B.C., Canada, V5A 1S6
glennc@ensc.sfu.ca, rmt3@sfu.ca

Israel Koren, Zahava Koren
Dept. of Electrical and Computer Engineering
University of Massachusetts
Amherst, MA, 01003
koren,zkoren@ecs.umass.edu

Abstract

Research has shown that in digital imaging sensors "Hot Pixels" defects accumulate as the camera ages over time. We have previously developed an empirical formula that projects hot pixel defects growth rates in terms of defect density (defects/year/mm²). We found that hot pixel densities grow via a power law, with the inverse of the pixel size raised to the power of about 3, and the ISO (gain) raised to the power of about 0.5. This paper experimentally explores the defect rates as pixels approach the 2 to 1 micron size. An analysis of the hot pixel parameters statistics shows that stuck high pixels that develop in the field are actually stuck hot pixels. In addition, this analysis indicates that as pixels shrink, not only does the defect rate increase, but it produces both a larger number of weak hot pixels at all ISOs, and a larger number of strong hot pixels at higher ISOs.

Keywords- imager defect detection, hot pixel development, APS/CCD defects rates, active pixel sensor APS, 1 micron pixels

INTRODUCTION

Digital imager technology now dominates the photographic field for both high end cameras and lower cost cellphone cameras. At the same time, it is becoming very common in embedded sensor design. Unfortunately, like any other integrated circuit device, digital imager sensors continuously develop defects over time. Differently than other microelectronic devices, most in-field defects in digital sensors begin appearing soon after fabrication, are permanent in nature and their number increases continuously over the lifetime of the sensor. These faulty pixels degrade the quality of the image captured by the sensor. Although the impact of defects can be overcome by recalibration, this can be expensive, is prone to errors, and is often infeasible for imagers used in remote sensing applications. This can create a serious problem in many applications where image quality and pixel sensitivity are important.

In our previous research, we have shown [1-6] that "Hot Pixels" are the most common type of defects that develop over time in modern digital imagers. Note that these are not fabrication time hot pixels (which are mapped out in most digital cameras) but defects that develop as the camera ages. Using statistical methods, we have shown that hot pixels are likely caused by cosmic rays [1-3]. The high energy of cosmic rays means that shielding or fabrication/design changes cannot fully prevent defect development with time. The exhibited strength of hot pixels increases with exposure time, but the underlying parameters remain constant after formation. We have developed an empirical formula, in the form of a power law, which relates the defect density D (defects per year per mm² of sensor area) to the pixel size S (in microns) and sensor gain (ISO). We discovered that D is proportional to the inverse of the pixel size raised to the third power, and to the square root of the gain. Therefore, as pixel sizes decrease by a factor of 2, the defect density D grows by about 8 times. This becomes extremely important as pixel sizes reduce to the 2-1 micron range seen in cellphones and many embedded devices. With a doubling of ISO, D increases by about 1.4 times.

In this paper, we analyze not just the number of hot pixels but also the distribution of their parameters as a function of pixel size and

sensitivity. With this analysis we gain an understanding of the growth model of defects, allowing us see where these new hot pixels are coming from as the pixel size gets smaller. As part of this work we show that new stuck high pixels, ones that are always saturated, are clearly partially stuck hot pixels, a fact that was indicated in previous research, but not proven.

Hot Pixels

In our previous research covering 12 years of data [5,6], we have performed manual calibrations on numerous commercial DSLRs, point and shoot cameras, and cellphone cameras. To identify defects, we used dark field exposures (i.e., no illumination) done at a range of exposure times (from 0.001 to 2 seconds) to test for stuck-high and partially stuck defects, and bright field (i.e., uniform illumination at near saturation) to test for stuck-low defects. In all of these experiments we did not find any truly stuck defects. Instead, hot pixels were the dominating defect type.

Under dark field (no illumination), a regular pixel shows almost no growth with increasing exposure time (see Figure 1). The dark response of both regular and hot pixels is demonstrated in Figure 1 showing the normalized pixel output versus exposure time (output level 0 represents no signal and 1 represents saturation). The dark response of a good pixel should be close to 0 (with some growth due to sensor noise) at any exposure time. By comparison, a classic hot pixel has a component that increases linearly with exposure time. In addition, we have found [5] that hot pixels can be categorized into two types: standard hot pixels, which have a component (dark current) that increases linearly with exposure time; and partially stuck or offset hot pixels which have a term that can be observed even at no exposure.
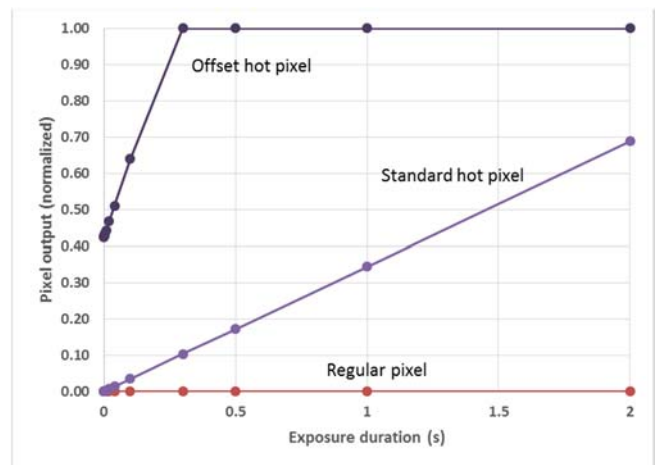
Figure 1: Comparing the dark response of imager pixels: a good regular pixel, a standard hot pixel, and an offset hot pixel.

The imaging sensor is often referred to as a digital system, but the actual pixel portion is an analog device. The classic assumed response of any pixel to illumination is given by equation (1), where I_{pix} is the response or output, R_{photo} is the incident illumination rate, R_{dark} is the

dark current rate, T_e is the duration of the exposure, b is the dark current offset, and m is the amplification from the ISO setting.

$$I_{pix}(R_{photo}, R_{dark}, T_e, b) = m*(R_{photo}\ T_e + R_{dark}\ T_e + b) \qquad (1)$$

For a good (regular) pixel, both dark current R_{dark} and offset b are, by design, as close to zero as the fabrication allows, so the output response gives a direct measure of the incident illumination. In a hot pixel, R_{dark} is significantly above the typical dark current noise level. This, combined with the offset b, creates an additional signal that adds to the incident illumination, making the pixel output higher (i.e., brighter in pictures). With zero illumination or dark frame testing the hot pixel offset model is shown in Equation (2).

$$I_{offset}(R_{dark}, T_e, b) = m*(R_{dark}\ T_e + b) \qquad (2)$$

The dark response in Equation (2), sometimes called the combined dark offset, is nearly linear in T_e. The parameters R_{dark} and b are extracted in our experiments by fitting a linear curve to the pixel dark frame response versus the exposure time, as seen in Figure 1. For standard hot pixels, the offset b is zero. These hot pixels are most visible in longer exposures (in the order of one second) as they do not have an initial offset. However, in the partially stuck hot pixel case, the magnitude of the offset b affects the response and this defect will appear as a bright spot in all images. In our research, testing each camera involves typically 5 to 20 dark images at a wide range of exposure times from 0.001 to 2 seconds and ISOs from the lowest to the highest values in the camera. The data is taken in digital RAW formats to minimize the impact of software adjustments which distort the measured values, such as demosaicing of the color image, JPEG spreading of defects and color correction [10]). To minimize sensor temperature effects, a 30 second delay is placed after each dark field image. We have developed a Matlab analysis program [2-4] to identify the hot pixels in each camera, and extract the pixel parameters and locations.
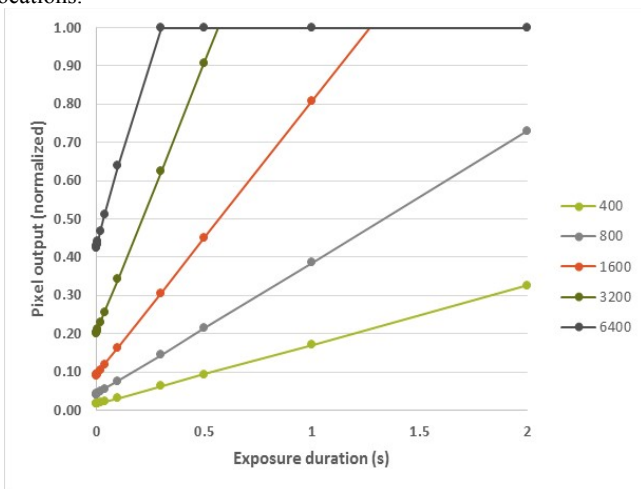
Figure 2: Dark response of one hot pixel at various ISO levels

The amplification of the pixel signal by the gain (ISO) setting also amplifies the values of both the hot pixel dark current R_{dark} and offset b. The measured values of the dark response for a typical hot pixel with increasing ISO levels is shown in Figure 2. At low ISO, most defects have smaller values of R_{dark} and b, though significantly above the background noise levels at longer exposures. As the ISO amplification increases, both R_{dark} and b increase dramatically, scaling linearly with the ISO (see Equation (1)). At ISO 12800 the dynamic range of the pixel is reduced by 40% solely due to the offset b, and at ISO 25600 the pixel is near saturation at all exposures. The significant number of hot

pixels with offsets has previously suggested to us that what seem to be stuck-high pixels, may actually be hot pixels with very high offsets.

The Origin of Stuck High Pixels

In any camera forum on the internet you will see discussions of cameras developing saturated stuck pixels. Yet in all of our experiments we have not detected a true stuck-high pixel in any of our cameras. What is the explanation for these differing observations?

We have tested cameras ranging from 29 DSLR cameras in the higher range pixel sizes (6 - 7 µm) with large sensors 340 to 860 mm^2 and ranging in age from 1 to 12 years, point-and-shoot cameras in the midrange pixel sizes (3 - 4 µm) with 20-40 mm^2 imagers, and cellphone cameras in the small pixel size range 2-3 µm and small sensors of 15-22 mm^2. From these we have been able to identify over 500 hot pixels, of which 44% were of the partially stuck type at *ISO* 400. Previously we had focused only on the defect density D. For this paper we developed new Matlab software that looked more deeply at the actual parameters (dark current and offset) of these hot pixels.

First, it is important to note that the ISO setting in an imager controls the amplification or sensitivity of the pixel output. Higher ISO settings enable objects to be captured under low light conditions or with very short exposures. This trend in camera designs to high ISO comes as it removes the need for flash photography or long exposure times when using natural light. At the beginning of digital photography years ago, most DSLRs had ISO of 100 – 1600. With improving sensor technology and better noise reduction algorithms, background noise levels have been reduced and the usable ISO range has increased considerably. Recent DSLRs have an ISO range of 50 to 12,300 and high-end cameras have a range from 25,600 to 409,600 ISO.

Previously we had assumed that it was the combination of dark current and offset b at longer exposures that were the source of the stuck hot pixels. However, when we carefully examined the actual hot pixel parameters we have observed something more interesting. We confined our interest to only hot pixels that eventually reach a saturated condition in the dark frame test. Typical results are shown for a 5 year old camera (with 6.3 um pixels) for dark current R_{dark} in Figure 3 and offset b in Figure 4 (a given pixel is shown for the same color in each figure).
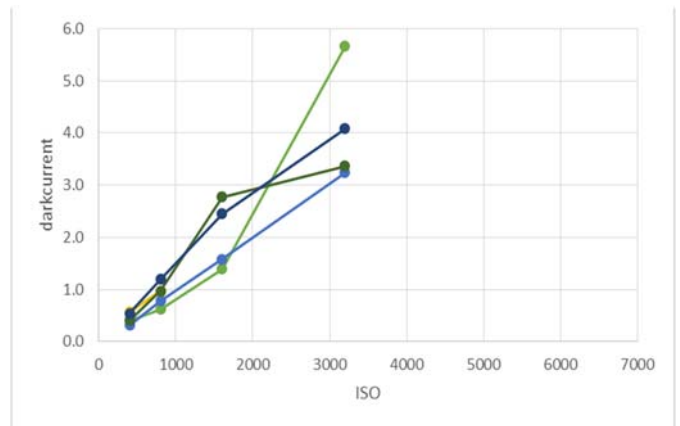
Figure 3: Dark current response of strong hot pixels vs ISO
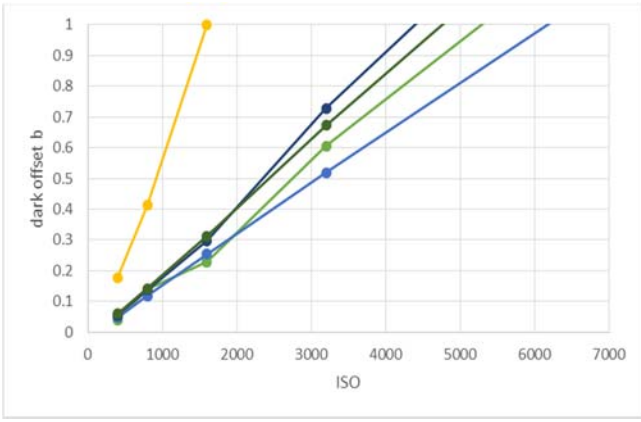
Figure 4: Dark offset b response of strong hot pixels vs ISO

As can be seen in Figure 3, the dark current increases rapidly with ISO. With a $R_{dark} = 1$ sec^{-1} the pixel would reach saturation at a one second exposure. All of these pixels exceed this value for ISOs in the 800 to 1600 range.

More importantly, Figure 4 shows the offset *b* for the same pixels. It is apparent that many of these pixels reach saturation at any exposure time (even 0.000125 seconds) at ISOs ranging from 1000 to 5000. As these are common levels for many cameras, these would appear to always be stuck at saturation.

When combined with the high dark currents of Figure 3, and noting that these hot pixels are also adding the photocurrent in regular exposures, many of these pixels reach saturation at even lower ISOs in regular photos. Hence, these partially stuck hot pixels have a greater impact on images than standard hot pixels as they are evident at any exposures even at modest ISOs.

This result was seen in every camera analyzed in our experiments (six cameras with pixel size ranging from 7.5 to 4.3 um) although, of course, the number of saturated pixels varied with pixel size, imager area, and camera age.

We cannot say for certain that all infield developed stuck high pixels reported in the literature are such offset hot pixels. What we can say is that every camera in our test group (29 cameras) did not exhibit stuck high hot pixels at all ISOs, but some did show stuck high pixels at many ISOs.

Defect Growth Rate

In our previous publications we have shown that hot pixel defects occurrences are randomly spaced across the imager [1-6]. Statistical analysis indicated that they are created by a random source such as cosmic rays [10]. The literature shows that other authors have reached a similar conclusion, and have argued that neutrons seem to create the same hot pixel defect types [7,8]. Using linear regression curve fitting to all our camera data over all ISOs we developed in [9,11] an empirical formula to relate the defect density *D* (defects per year per mm^2 of sensor area) to the pixel size *S* (in microns) and sensor gain (ISO) via the following equations:

For APS pixels:

$$D=10^{-1.12}S^{-3.15}ISO^{0.525} \qquad (3)$$

For CCD sensors

$$D=10^{-1.849}S^{-2.25}ISO^{0.687} \qquad (4)$$

Figure 5 shows a plot of Equation (3) for the full test range. These equations indicate that the defect density increases drastically when the pixel size falls below 2 microns (see Figure 6), and is projected to reach 12.5 defects/year/mm^2 at ISO 25,600 (which is already available on some high-end cameras).

Since the current trend is to further reduce the size of pixels, these experimental results project that the number of these defects will increase to high levels, emphasizing the need to understand how the development rate of these defects increases as the pixel size reduces.
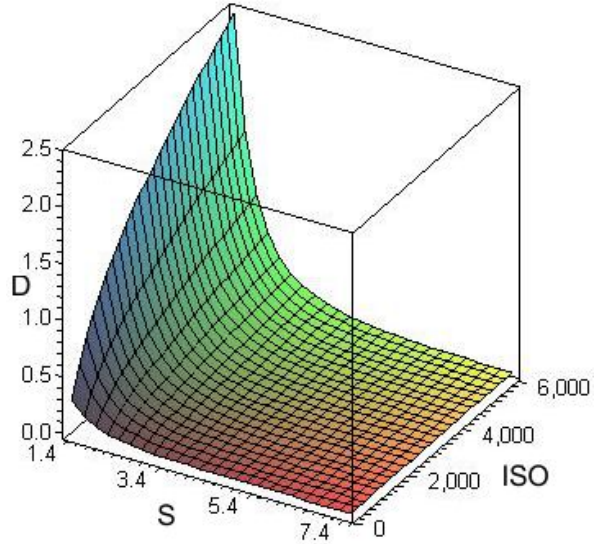
Figure 5: Fitted power law for APS: defect density (D=defects/year/mm²) vs. pixel size S (µm) and ISO (I)
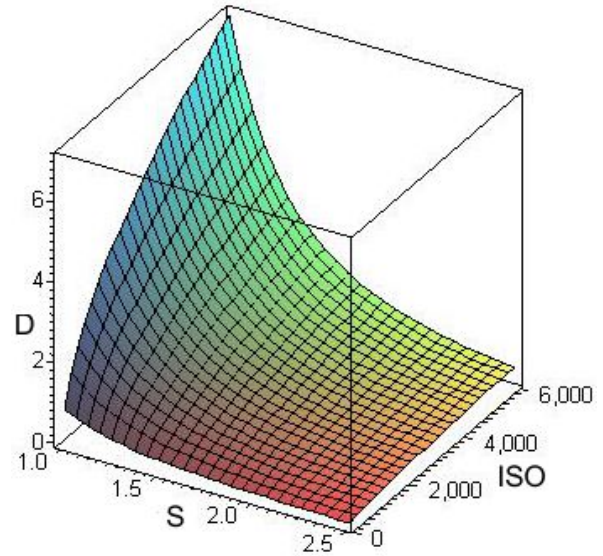
Figure 5: Fitted power law for APS in the 1 to 2.5 µm pixel range: defect density (D=defects/year/mm2) vs. pixel size S (µm) and ISO (I)
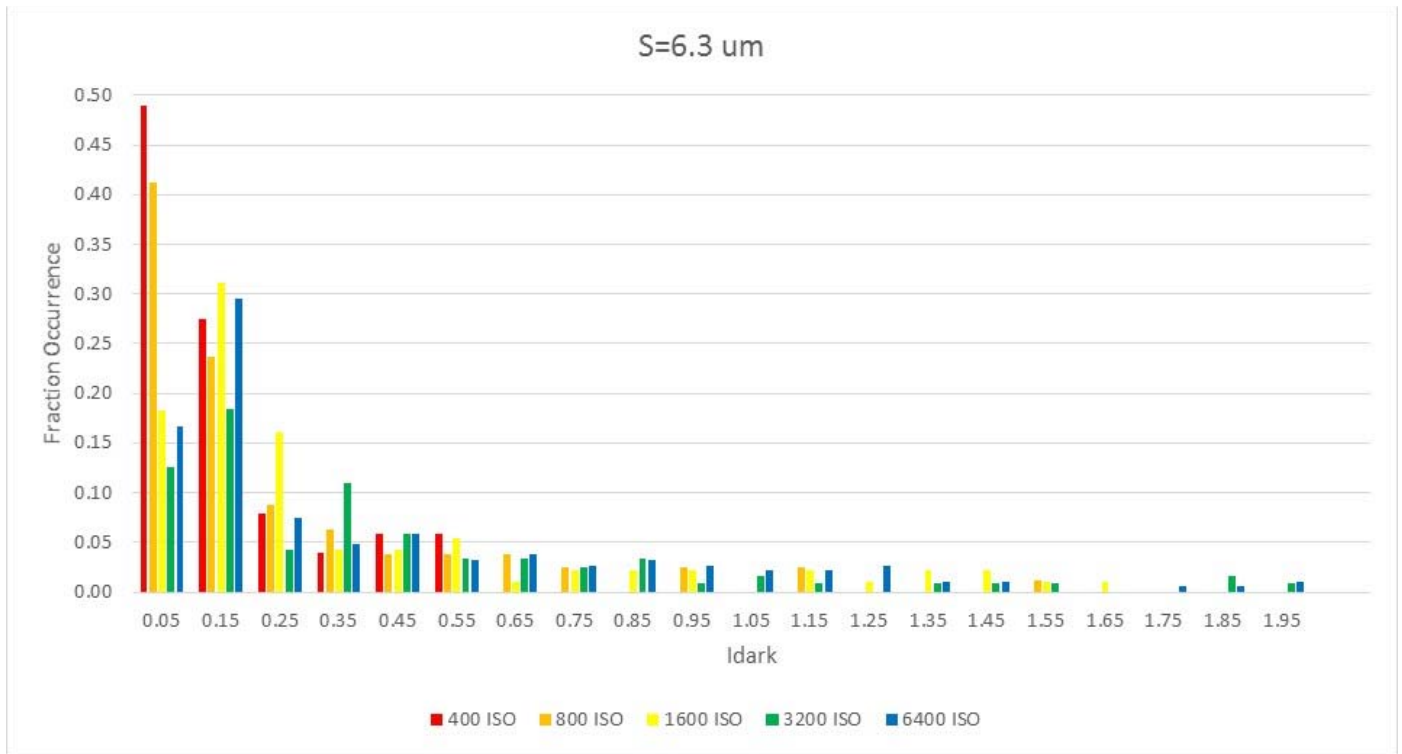
Figure 6: Fraction of defects vs dark current R$_{dark}$ for 6.3µm pixels
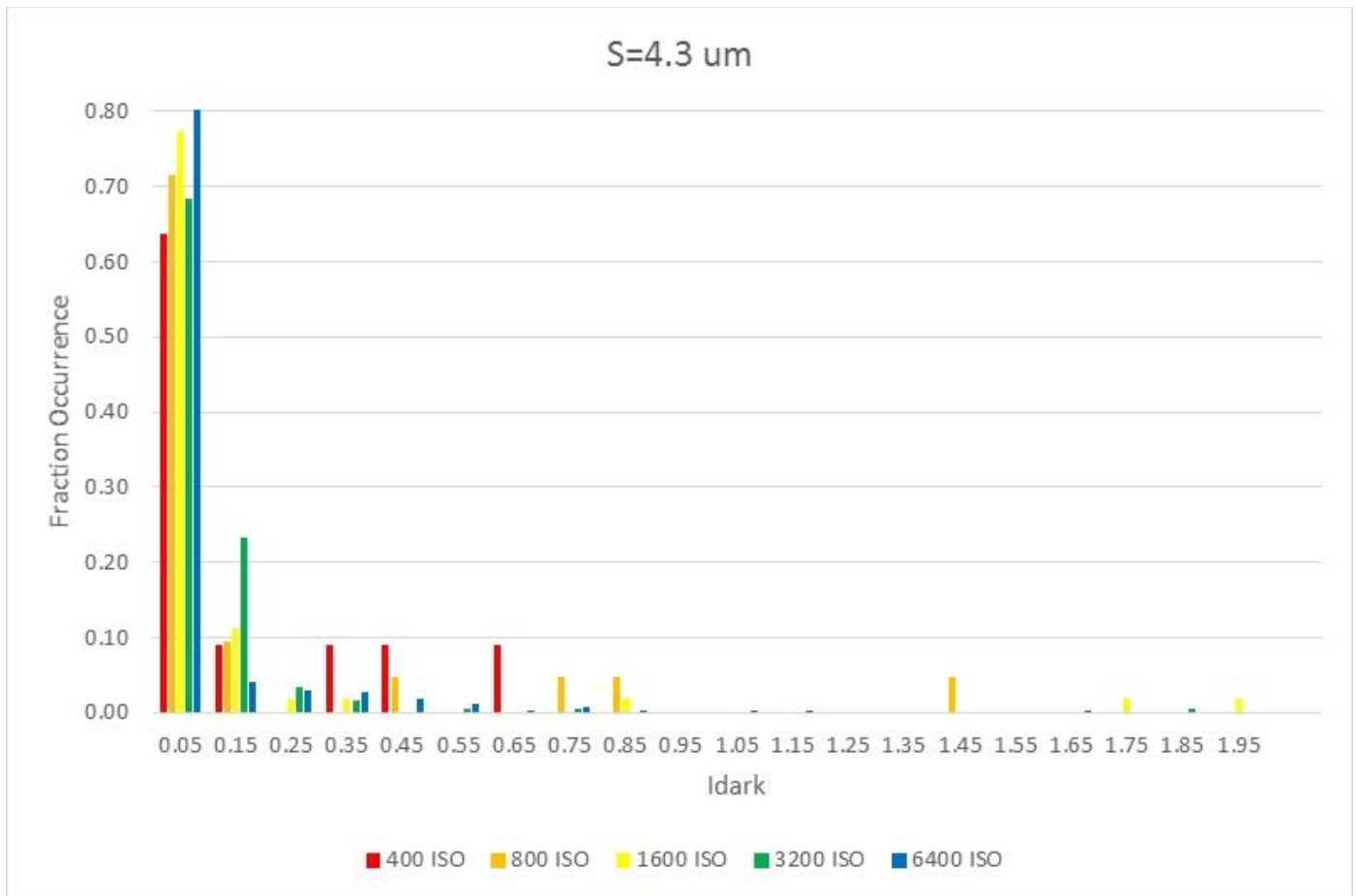
Figure 7: Fraction of defects vs dark current R$_{dark}$ for 4.3µm pixels
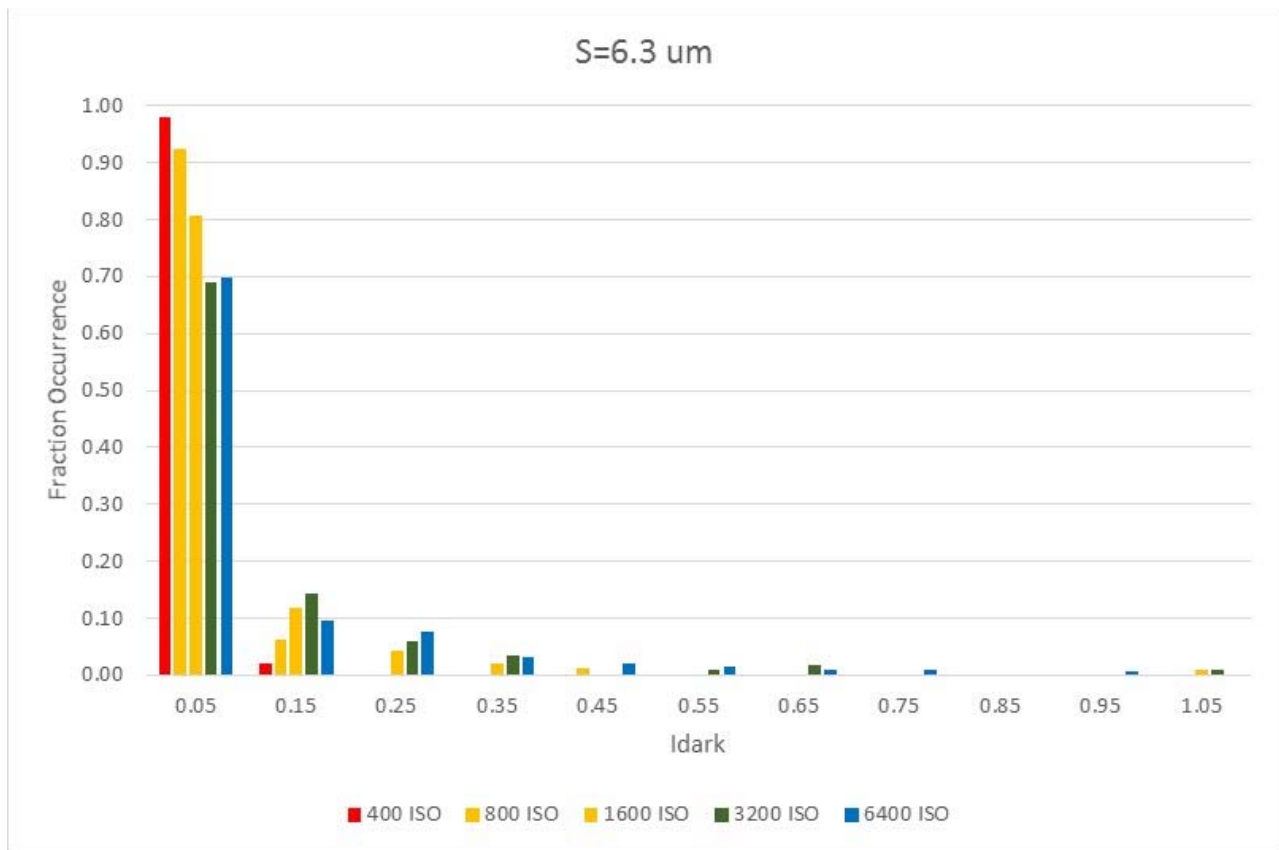
Figure 8: Fraction of defects vs offset b for 6.3µm pixels
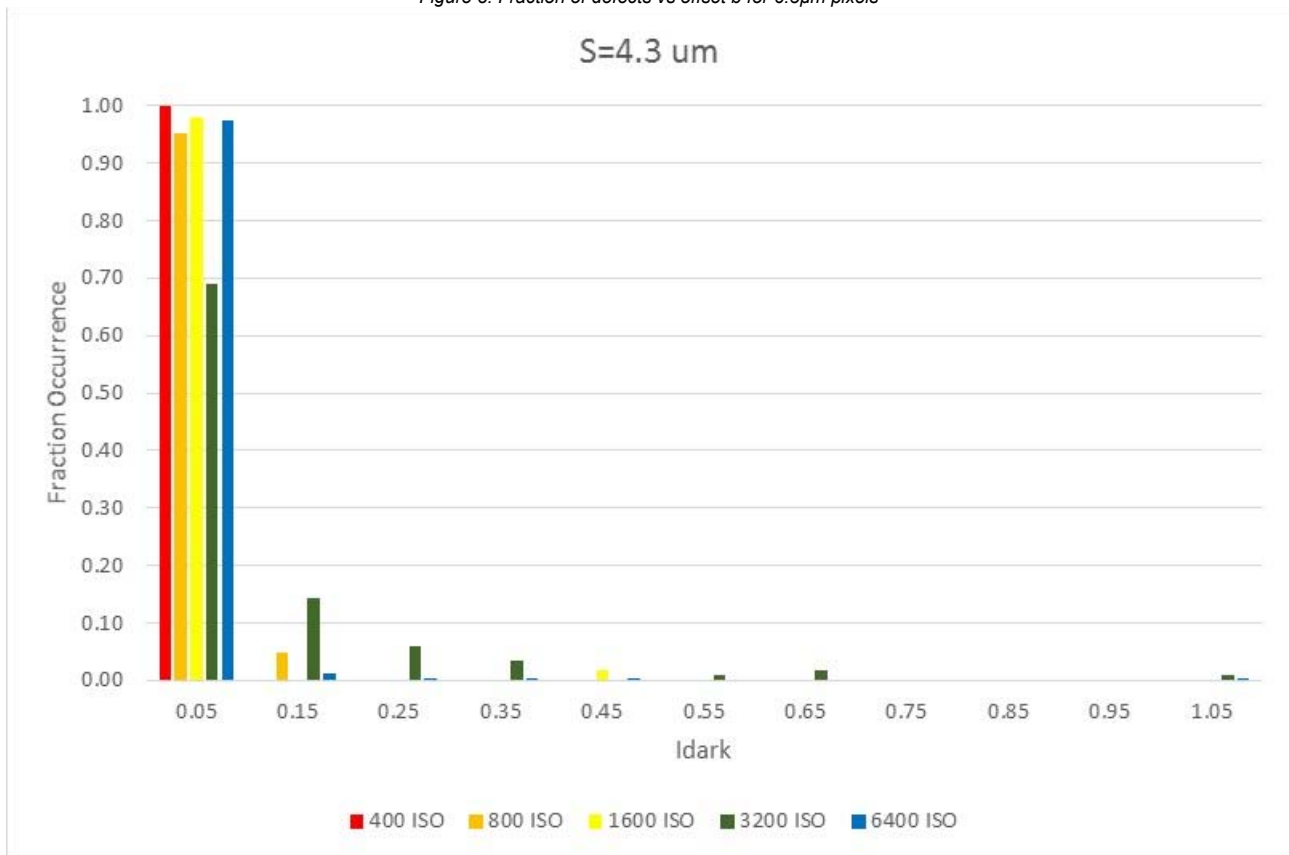
Figure 9: Fraction of defects vs offset b for 4.3µm pixels

Hot Pixel Parameters and Defect Growth Rate

In previously reported research [5] we showed that the size of the hot pixel created defect is very small, less than 5% of the pixel size.

By assuming that the damaged point that creates the hot pixel is independent of the actual size of the pixel, we would expect that as the pixel shrinks, the defect rate would scale with the reduction in the pixel area, S^2. Still, our current formula (Equation 3) suggests that a shrinkage of the pixel size by a factor of 2 results in an 8.9 times increase in the defect rate, which is the pixel size to about the 3rd power. Higher imager sensitivities (ISOs) increase this effect by the square root of the increase in ISO. To understand the reason behind it, we look at what the hot pixel measurements tell us about the distribution of the pixel parameters.

Figures 6-7 compare the hot pixel dark current distributions of two cameras with 6.3 um and 4.3 um pixels over ISOs from 400 to 6400 values (these cameras are respectively 5 and 4 years old). In these figures, bins are 0.1 sec^{-1} wide and are centered at the 0.05 sec^{-1} bin point. Vertical axes show the fraction of hot pixels with the corresponding dark current.

Note the significant difference in the distribution of dark current in all ISOs for these two pixel sizes. S=6.3 pixels in Figure 6 start with a high fraction of the pixels at the lowest bin but as ISO rises, these weaker pixels get amplified to higher bins to be replaced by a smaller fraction of new weak pixels. At ISO 400, 0.49 of the hot pixels are in the lowest bin but by comparison, at 6400 ISO this is down to only 0.15 of the hot pixels.

By comparison, at S=4.3 um (Figure 7) the fraction of the lowest bin weaker pixels is much higher, 0.65, at ISO 400, and by ISO 6400 rises to 0.85, some 5.6 times higher than for the 6.3um pixels. This means that many more new hot pixels are added to the lowest bin for the smaller pixel camera.

However, this does not mean that the smaller pixel camera only creates very weak hot pixels. If we look at the defect density D for both cameras something interesting appears. Table 1 gives D for all ISOs in these cameras. This shows that D is greater for all ISOs larger than 1600, for the 4.3 um pixels than for the 6.3 um pixels and at 6400 ISO, it is nearly 10 times higher.

Table 1: Defect Density D (Defects/mm^2/year) for various ISO values at pixel sizes S = 6.3um and 4.3um

ISO	S=6.3um	S=4.3um
400	0.011	0.012
800	0.015	0.014
1600	0.017	0.036
3200	0.021	0.109
6400	0.026	0.249

Table 2: Defect rate greater than minimum Rate D+ (Defects/mm^2/year) for various ISOs at pixel sizes S= 6.3um and 4.3um

ISO	S=6.3um	S=4.3um
400	0.0056	0.0044
800	0.0086	0.0040
1600	0.0139	0.0094
3200	0.0184	0.0349
6400	0.0217	0.0423

In Table 2 we show the effective rate D for hot pixels in all the bins above the bottom (i.e., stronger hot pixels). What we see is that at 6400 ISO the effective high dark current rate D for the 4.3 um imager is twice that of the 6.3 um pixel camera. This means that not only are more hot pixels added, but there are more strong hot pixels at the higher rate.

Looking at the hot pixel offset b for these two cameras in Figures 8-9 we see a different trend. In these plots a bin of, say 0.25, means that the pixels start for all exposures with a 25% of saturation value which would make them quite noticeable. For the 6.3 micron camera (Figure 8) we again see that the offsets are even more concentrated (98%) in the lowest bin (i.e., values nearly zero) at ISO 400. As the gain increases, the fraction in the lowest bin declines while again there is a spreading out of the offsets to the higher bins. By 3200 and 6400 ISO, nearly 30% of the pixels are in the higher bins. Note that for 3200 and 6400 there are about 3% of the pixels at b=1.0 which means that they are true stuck high (saturated) pixels.

For the 4.3 micron pixels (Figure 9), the offset also shows that with increasing gain most of the new pixels appear in the lowest offset bin. The spread to the higher bins (stronger offsets) is less here, and only 1% of the pixels reach saturation at the highest ISOs.

Note that while these results are for two particular cameras, very similar distributions were observed for other cameras of the same pixel range.
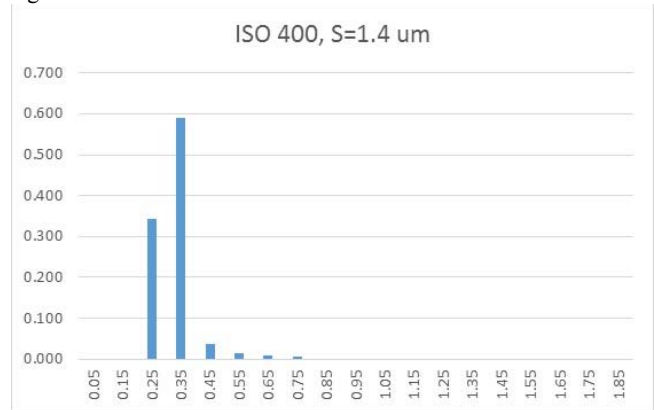
Figure 10: Defect distribution vs dark current R_{dark} for 1.4µm pixels at 400 ISO
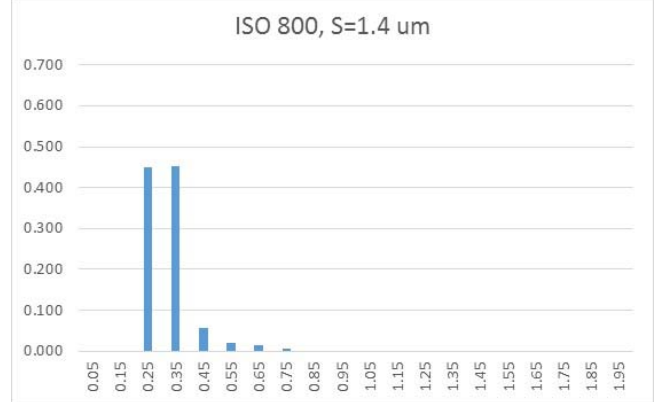
Figure 11: Defect distribution vs dark current R_{dark} for 1.4µm pixels at 800 ISO

To study pixels in the 2 to 1 micron range it is necessary to use cellphone cameras. As noted in our previous research [11], only a few of the newest Android OS phones support digital RAW file output needed for this research. These RAW images are quite noisy, making the identification and analysis of hot pixels a difficult task. Since cell phones sensors heat rapidly, we need to fully turn off the phone and let it cool to room temperature before turning it on for the next test. This is due to the inherent lack of noise suppression algorithms in cellphone imagers as compared to those used in DSLR cameras. We have developed specialized detection algorithms that enable us to obtain a defect count for various cell phone imagers. We also ensured that hot pixel detections in cellphone cameras are statistically significant within the error margins. The analysis requires that either the fitted offset or dark current is statistically significant before the hot pixel is regarded

as a true hot pixel. If neither is significant, then it will be considered as noise. Finally, while cellphone manufactures do allow their cameras to have a 400 to 3200 ISO range, the noise levels above 800 ISO are so great that it is impossible to separate the hot pixels from the background. Even for this lower ISO the smallest bin (0.15) is too close to the noise level to detect hot pixels.

Figures 10-11 show a trend similar to that observed for the 4.3 um cameras – most of the dark current is in the lowest detectable bins, and there is a very limited spreading of pixels to higher dark currents as the gain increases. It is notable that the 800 ISO 1.4 um pixel results show almost twice the number of hot pixels as the 400 ISO measurements, indicating again that new hot pixels which appear with an increasing gain are from weak defects that rise above the noise, as happens in the DSLR tests.

The number of cell phones supporting the RAW format was limited in this student. Fortunately the latest series of higher end cellphones now often include digital RAW output possibilities in their cameras. This will give us more data for this analysis in the near future

Conclusions

In this paper, we have moved from merely counting the hot pixels and analyzing their development rates, to using the hot pixel parameter distributions to try and understand why the rates are increasing as pixels shrink. The first result of analyzing the hot pixel parameter statistics shows that stuck high pixels are really hot pixels with a strong offset.

The parameter analysis also shows that smaller pixels produce both higher rates of defects and higher fractions of weaker hot pixels. The strongest hot pixels grow in numbers, but not in percentage. We are using this to gain a better understanding of why the hot pixel defect rate increases with at a power of S^{-3} rate rather than just scaling with the pixel area.

References

[1] J. Dudas, L.M. Wu, C. Jung, G.H. Chapman, Z. Koren, and I. Koren, "Identification of in-field defect development in digital image sensors," *Proc. Electronic Imaging, Digital Photography III*, v6502, 65020Y1-0Y12, San Jose, Jan 2007.

[2] J. Leung, G.H. Chapman, I. Koren, and Z. Koren, "Statistical Identification and Analysis of Defect Development in Digital Imagers," *Proc. SPIE Electronic Imaging, Digital Photography V*, v7250, 742903-1 – 03-12, San Jose, Jan 2009.

[3] J. Leung, G. Chapman, I. Koren, and Z. Koren, "Automatic Detection of In-field Defect Growth in Image Sensors," *Proc. of the 2008 IEEE Intern. Symposium on Defect and Fault Tolerance in VLSI Systems*, 220-228, Boston, MA, Oct. 2008.

[4] J. Leung, G. H. Chapman, I. Koren, Z. Koren, "Tradeoffs in imager design with respect to pixel defect rates," *Proc. of the 2010 Intern. Symposium on Defect and Fault Tolerance in VLSI*, 231-239., Kyoto, Japan, Oct 2010.

[5] J. Leung, J. Dudas, G. H. Chapman, I. Koren, Z. Koren, "Quantitative Analysis of In-Field Defects in Image Sensor Arrays," *Proc. 2007 Intern. Sym on Defect and Fault Tolerance in VLSI*, 526-534, Rome, Italy, Sept 2007.

[6] J. Leung, G.H. Chapman, Y.H. Choi, R. Thomson, I. Koren, and Z. Koren, "Tradeoffs in imager design parameters for sensor reliability," *Proc., Electronic Imaging, Sensors, Cameras, and Systems for Industrial/Scientific Applications XI*, v 7875, 78750I1-0I12, San Jose, Jan. 2011.

[7] A.J.P. Theuwissen, "Influence of terrestrial cosmic rays on the reliability of CCD image sensors. Part 1: experiments at room temperature," *IEEE Transactions on Electron Devices*, Vol. 54 (12), 3260-6, 2007.

[8] A.J.P. Theuwissen, "Influence of terrestrial cosmic rays on the reliability of CCD image sensors. Part 2: experiments at elevated temperature," *IEEE Transactions on Electron Devices*, Vol. 55 (9), 2324-8, 2008.

[9] G.H. Chapman, R. Thomas, I. Koren, and Z. Koren, "Empirical formula for rates of hot pixel defects based on pixel size, sensor area and ISO", *Proc. Electronic Imaging, Sensors, Cameras, and Systems for Industrial/Scientific Applications XIII*, v8659, 86590C-1-C-11 San Francisco, Jan. 2013.

[10] J. Leung, "Measurement and Analysis of Defect Development in Digital Imagers, MASc thesis, Simon Fraser University, School of Engineering Science, Burnaby, BC Canada, 2011.

[11] G.H. Chapman, R. Thomas, K.J. Meneses, T.Q. Yang, I. Koren, and Z. Koren, "Increases in Hot Pixel Development Rates for Small Digital Pixel Sizes", *Proc. Electronic Imaging, Sensors, Cameras, and Systems for Industrial/Scientific Applications XIX*, San Francisco, Feb. 2015.

Author Biographies

Glenn Chapman, Professor, School of Engineering Science, Simon Fraser University, Canada, researching in defects in digital image sensors. BSc and MSc Physics Queen's University, and PhD McMaster University, Canada.

Israel Koren, Professor, Electrical and Computer Engineering at the University of Massachusetts, Amherst and a fellow of the IEEE. BSc, MSc and DSc Technion - Israel Institute of Technology.

Zahava Koren, senior researcher, University of Massachusetts, Amherst. B.A and M.A degrees in Mathematics and Statistics, Hebrew University, Jerusalem, and D.Sc. degree Operations Research, Technion - Israel Institute of Technology.